

TrackFormer: Multi-Object Tracking with Transformers

Tim Meinhardt¹ *

Alexander Kirillov²

Laura Leal-Taixé¹

Christoph Feichtenhofer²

¹Technical University of Munich

²Facebook AI Research (FAIR)

Abstract

The challenging task of multi-object tracking (MOT) requires simultaneous reasoning about track initialization, identity, and spatio-temporal trajectories. We formulate this task as a frame-to-frame set prediction problem and introduce TrackFormer, an end-to-end trainable MOT approach based on an encoder-decoder Transformer architecture. Our model achieves data association between frames via attention by evolving a set of track predictions through a video sequence. The Transformer decoder initializes new tracks from static object queries and autoregressively follows existing tracks in space and time with the conceptually new and identity preserving track queries. Both query types benefit from self- and encoder-decoder attention on global frame-level features, thereby omitting any additional graph optimization or modeling of motion and/or appearance. TrackFormer introduces a new tracking-by-attention paradigm and while simple in its design is able to achieve state-of-the-art performance on the task of multi-object tracking (MOT17 and MOT20) and segmentation (MOTS20). The code is available at <https://github.com/timmeinhardt/trackformer>.

1. Introduction

Humans need to focus their *attention* to track objects in space and time, for example, when playing a game of tennis, golf, or pong. This challenge is only increased when tracking not one, but *multiple* objects, in crowded and real world scenarios. Following this analogy, we demonstrate the effectiveness of Transformer [51] attention for the task of multi-object tracking (MOT) in videos.

The goal in MOT is to follow the trajectories of a set of objects, *e.g.*, pedestrians, while keeping their identities discriminated as they are moving throughout a video sequence. Due to the advances in image-level object detection [7, 39], most approaches follow the two-step *tracking-by-detection* paradigm: (i) detecting objects in individual video frames,

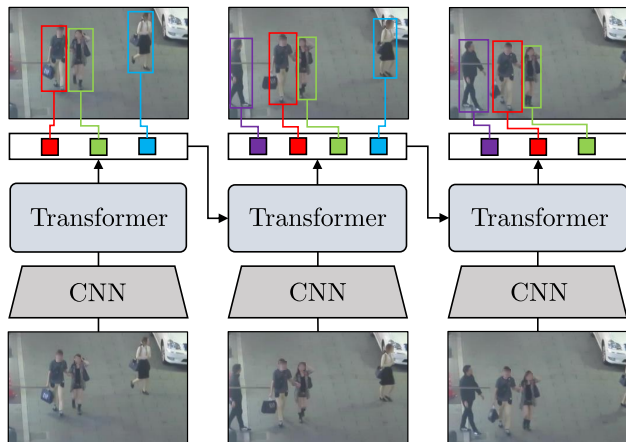


Figure 1. TrackFormer jointly performs object detection and tracking-by-attention with Transformers. Object and autoregressive track queries reason about track initialization, identity, and spatiotemporal trajectories.

and (ii) associating sets of detections between frames and thereby creating individual object tracks over time. Traditional tracking-by-detection methods associate detections via temporally sparse [23, 26] or dense [19, 22] graph optimization, or apply convolutional neural networks to predict matching scores between detections [8, 24].

Recent works [4, 6, 29, 69] suggest a variation of the traditional paradigm, coined *tracking-by-regression* [12]. In this approach, the object detector not only provides frame-wise detections, but replaces the data association step with a continuous regression of each track to the changing position of its object. These approaches achieve track association implicitly, but provide top performance only by relying either on additional graph optimization [6, 29] or motion and appearance models [4]. This is largely due to the isolated and local bounding box regression which lacks any notion of object identity or global communication between tracks.

In this work, we introduce the *tracking-by-attention* paradigm which not only applies attention for data association [11, 70] but jointly performs tracking and detection. As shown in Figure 1, this is achieved by evolving a set of

*Work done during an internship at Facebook AI Research.
Correspondence to: tim.meinhardt@tum.de

tracks from frame to frame forming trajectories over time.

We present a first straightforward instantiation of tracking-by-attention, TrackFormer, an end-to-end trainable Transformer [51] encoder-decoder architecture. It encodes frame-level features from a convolutional neural network (CNN) [18] and decodes queries into bounding boxes associated with identities. The data association is performed through the novel and simple concept of *track queries*. Each query represents an object and follows it in space and time over the course of a video sequence in an autoregressive fashion. New objects entering the scene are detected by static object queries as in [7, 71] and subsequently transform to future track queries. At each frame, the encoder-decoder computes attention between the input image features and the track as well as object queries, and outputs bounding boxes with assigned identities. Thereby, TrackFormer performs tracking-by-attention and achieves detection and data association jointly without relying on any additional track matching, graph optimization, or explicit modeling of motion and/or appearance. In contrast to tracking-by-detection/regression, our approach detects and associates tracks simultaneously in a single step via attention (and not regression). TrackFormer extends the recently proposed set prediction objective for object detection [7, 48, 71] to multi-object tracking.

We evaluate TrackFormer on the MOT17 [30] and MOT20 [13] benchmarks where it achieves state-of-the-art performance for public and private detections. Furthermore, we demonstrate the extension with a mask prediction head and show state-of-the-art results on the Multi-Object Tracking and Segmentation (MOTS20) challenge [52]. We hope this simple yet powerful baseline will inspire researchers to explore the potential of the tracking-by-attention paradigm.

In summary, we make the following contributions:

- An end-to-end trainable multi-object tracking approach which achieves detection and data association in a new tracking-by-attention paradigm.
- The concept of autoregressive track queries which embed an object’s spatial position and identity, thereby tracking it in space and time.
- New state-of-the-art results on three challenging multi-object tracking (MOT17 and MOT20) and segmentation (MOTS20) benchmarks.

2. Related work

In light of the recent trend in MOT to look beyond tracking-by-detection, we categorize and review methods according to their respective tracking paradigm.

Tracking-by-detection approaches form trajectories by associating a given set of detections over time.

Graphs have been used for track association and long-term re-identification by formulating the problem as a maximum flow (minimum cost) optimization [3] with distance based [21, 37, 64] or learned costs [25]. Other methods use association graphs [46], learned models [23], and motion information [22], general-purpose solvers [63], multi-cuts [49], weighted graph labeling [19], edge lifting [20], or trainable graph neural networks [6, 55]. However, graph-based approaches suffer from expensive optimization routines, limiting their practical application for online tracking.

Appearance driven methods capitalize on increasingly powerful image recognition backbones to track objects by relying on similarity measures given by twin neural networks [24], learned reID features [33, 42], detection candidate selection [8] or affinity estimation [10]. Similar to re-identification, appearance models struggle in crowded scenarios with many object-object-occlusions.

Motion can be modelled for trajectory prediction [1, 26, 43] using a constant velocity assumption (CVA) [2, 9] or the social force model [26, 35, 44, 59]. Learning a motion model from data [25] accomplishes track association between frames [65]. However, the projection of non-linear 3D motion [50] into the 2D image domain still poses a challenging problem for many models.

Tracking-by-regression refrains from associating detections between frames but instead accomplishes tracking by regressing past object locations to their new positions in the current frame. Previous efforts [4, 15] use regression heads on region-pooled object features. In [69], objects are represented as center points which allow for an association by a distance-based greedy matching algorithm. To overcome their lacking notion of object identity and global track reasoning, additional re-identification and motion models [4], as well as traditional [29] and learned [6] graph methods have been necessary to achieve top performance.

Tracking-by-segmentation not only predicts object masks but leverages the pixel-level information to mitigate issues with crowdedness and ambiguous backgrounds. Prior attempts used category-agnostic image segmentation [31], applied Mask R-CNN [17] with 3D convolutions [52], mask pooling layers [38], or represented objects as unordered point clouds [58] and cost volumes [57]. However, the scarcity of annotated MOT segmentation data makes modern approaches still rely on bounding boxes.

Attention for image recognition correlates each element of the input with respect to the others and is used in Transformers [51] for image generation [34] and object detection [7, 71]. For MOT, attention has only been used to associate a given set of object detections [11, 70], not tackling the detection and tracking problem jointly.

In contrast, TrackFormer casts the entire tracking objective into a single set prediction problem, applying attention not only for the association step. It jointly reasons about track initialization, identity, and spatio-temporal trajectories. We only rely on feature-level attention and avoid additional graph optimization and appearance/motion models.

3. TrackFormer

We present TrackFormer, an end-to-end trainable multi-object tracking (MOT) approach based on an encoder-decoder Transformer [51] architecture. This section describes how we cast MOT as a set prediction problem and introduce the new *tracking-by-attention* paradigm. Furthermore, we explain the concept of *track queries* and their application for frame-to-frame data association.

3.1. MOT as a set prediction problem

Given a video sequence with K individual object identities, MOT describes the task of generating ordered tracks $T_k = (b_{t_1}^k, b_{t_2}^k, \dots)$ with bounding boxes b_t and track identities k . The subset (t_1, t_2, \dots) of total frames T indicates the time span between an object entering and leaving the scene. These include all frames for which an object is occluded by either the background or other objects.

In order to cast MOT as a set prediction problem, we leverage an encoder-decoder Transformer architecture. Our model performs online tracking and yields per-frame object bounding boxes and class predictions associated with identities in four consecutive steps:

- (i) Frame-level feature extraction with a common CNN backbone, *e.g.*, ResNet-50 [18].
- (ii) Encoding of frame features with self-attention in a Transformer encoder [51].
- (iii) Decoding of queries with self- and encoder-decoder attention in a Transformer decoder [51].
- (iv) Mapping of queries to box and class predictions using multilayer perceptrons (MLP).

Objects are implicitly represented in the decoder *queries*, which are embeddings used by the decoder to output bounding box coordinates and class predictions. The decoder alternates between two types of attention: (i) self-attention over all queries, which allows for joint reasoning about the objects in a scene and (ii) encoder-decoder attention, which gives queries global access to the visual information of the encoded features. The output embeddings accumulate bounding box and class information over multiple decoding layers. The permutation invariance of Transformers requires additive feature and object encodings for the frame features and decoder queries, respectively.

3.2. Tracking-by-attention with queries

The total set of output embeddings is initialized with two types of query encodings: (i) static object queries, which allow the model to initialize tracks at any frame of the video, and (ii) autoregressive track queries, which are responsible for tracking objects across frames.

The simultaneous decoding of object and track queries allows our model to perform detection and tracking in a unified way, thereby introducing a new *tracking-by-attention* paradigm. Different tracking-by-X approaches are defined by their key component responsible for track generation. For tracking-by-detection, the tracking is performed by computing/modelling distances between frame-wise object detections. The tracking-by-regression paradigm also performs object detection, but tracks are generated by regressing each object box to its new position in the current frame. Technically, our TrackFormer also performs regression in the mapping of object embeddings with MLPs. However, the actual track association happens earlier via attention in the Transformer decoder. A detailed architecture overview which illustrates the integration of track and object queries into the Transformer decoder is shown in the appendix.

Track initialization. New objects appearing in the scene are detected by a fixed number of N_{object} output embeddings each initialized with a static and learned object encoding referred to as *object queries* [7]. Intuitively, each object query learns to predict objects with certain spatial properties, such as bounding box size and position. The decoder self-attention relies on the object encoding to avoid duplicate detections and to reason about spatial and categorical relations of objects. The number of object queries is ought to exceed the maximum number of objects per frame.

Track queries. In order to achieve frame-to-frame track generation, we introduce the concept of *track queries* to the decoder. Track queries follow objects through a video sequence carrying over their identity information while adapting to their changing position in an autoregressive manner.

For this purpose, each new object detection initializes a track query with the corresponding output embedding of the previous frame. The Transformer encoder-decoder performs attention on frame features and decoder queries *continuously updating* the instance-specific representation of an object’s identity and location in each track query embedding. Self-attention over the joint set of both query types allows for the detection of new objects while simultaneously avoiding re-detection of already tracked objects.

In Figure 2, we provide a visual illustration of the track query concept. The initial detections in frame $t = 0$ spawn new track queries following their corresponding objects to frame t and beyond. To this end, N_{object} ob-

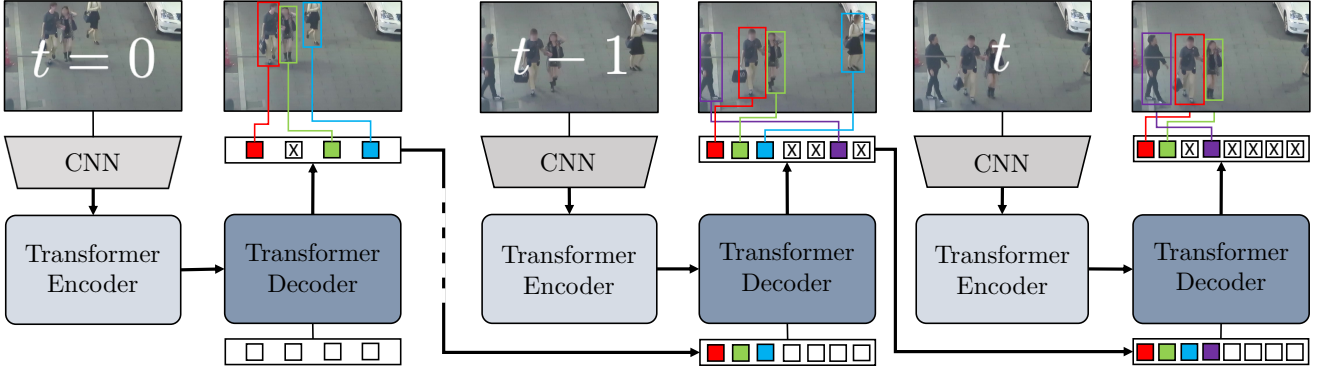


Figure 2. **TrackFormer** casts multi-object tracking as a set prediction problem performing joint detection and **tracking-by-attention**. The architecture consists of a CNN for image feature extraction, a Transformer [51] encoder for image feature encoding and a Transformer decoder which applies self- and encoder-decoder attention to produce output embeddings with bounding box and class information. At frame $t = 0$, the decoder transforms N_{object} object queries (white) to output embeddings either initializing new autoregressive **track queries** or predicting the background class (crossed). On subsequent frames, the decoder processes the joint set of $N_{\text{object}} + N_{\text{track}}$ queries to follow or remove (blue) existing tracks as well as initialize new tracks (purple).

ject queries (white) are decoded to output embeddings for potential track initializations. Each valid object detection $\{b_0^0, b_0^1, \dots\}$ with a classification score above σ_{object} , *i.e.*, output embedding not predicting the background class (crossed), initializes a new track query embedding. Since not all objects in a sequence appear on the first frame, the track identities $K_{t=0} = \{0, 1, \dots\}$ only represent a subset of all K . For the decoding step at any frame $t > 0$, track queries initialize additional output embeddings associated with different identities (colored). The joint set of $N_{\text{object}} + N_{\text{track}}$ output embeddings is initialized by (learned) object and (temporally adapted) track queries, respectively.

The Transformer decoder transforms the entire set of output embeddings at once and provides the input for the subsequent MLPs to predict bounding boxes and classes for frame t . The number of track queries N_{track} changes between frames as new objects are detected or tracks removed. Tracks and their corresponding query can be removed either if their classification score drops below σ_{track} or by non-maximum suppression (NMS) with an IoU threshold of σ_{NMS} . A comparatively high σ_{NMS} only removes strongly overlapping duplicate bounding boxes which we found to not be resolvable by the decoder self-attention.

Track query re-identification. The ability to decode an arbitrary number of track queries allows for an attention-based short-term re-identification process. We keep decoding previously removed track queries for a maximum number of $T_{\text{track-reid}}$ frames. During this *patience window*, track queries are considered to be inactive and do not contribute to the trajectory until a classification score higher than $\sigma_{\text{track-reid}}$ triggers a re-identification. The spatial information embedded into each track query prevents their application for long-term occlusions with large object movement, but,

nevertheless, allows for a short-term recovery from track loss. This is possible without any dedicated re-identification training; and furthermore, cements TrackFormer’s holistic approach by relying on the same attention mechanism as for track initialization, identity preservation and trajectory forming even through short-term *occlusions*.

3.3. TrackFormer training

For track queries to work in interaction with object queries and follow objects to the next frame, TrackFormer requires dedicated frame-to-frame tracking training. As indicated in Figure 2, we train on two adjacent frames and optimize the entire MOT objective at once. The loss for frame t measures the set prediction of all output embeddings $N = N_{\text{object}} + N_{\text{track}}$ with respect to the ground truth objects in terms of class and bounding box prediction.

The set prediction loss is computed in two steps:

- (i) Object detection on frame $t - 1$ with N_{object} object queries (see $t = 0$ in Figure 2).
- (ii) Tracking of objects from (i) and detection of new objects on frame t with all N queries.

The number of track queries N_{track} depends on the number of successfully detected objects in frame $t - 1$. During training, the MLP predictions $\hat{y} = \{\hat{y}_j\}_{j=1}^N$ of the output embeddings from step (iv) are each assigned to one of the ground truth objects y or the background class. Each y_i represents a bounding box b_i , object class c_i and identity k_i .

Bipartite matching. The mapping $j = \pi(i)$ from ground truth objects y_i to the joint set of object and track query predictions \hat{y}_j is determined either via track identity or costs based on bounding box similarity and object class. For the

former, we denote the subset of ground truth track identities at frame t with $K_t \subset K$. Each detection from step (i) is assigned to its respective ground truth track identity k from the set $K_{t-1} \subset K$. The corresponding output embeddings, *i.e.*, track queries, inherently carry over the identity information to the next frame. The two ground truth track identity sets describe a hard assignment of the N_{track} track query outputs to the ground truth objects in frame t :

$K_t \cap K_{t-1}$: Match by track identity k .

$K_{t-1} \setminus K_t$: Match with background class.

$K_t \setminus K_{t-1}$: Match by minimum cost mapping.

The second set of ground truth track identities $K_{t-1} \setminus K_t$ includes tracks which either have been occluded or left the scene at frame t . The last set $K_{\text{object}} = K_t \setminus K_{t-1}$ of previously not yet tracked ground truth objects remains to be matched with the N_{object} object queries. To achieve this, we follow [7] and search for the injective minimum cost mapping $\hat{\sigma}$ in the following assignment problem,

$$\hat{\sigma} = \arg \min_{\sigma} \sum_{k_i \in K_{\text{object}}} C_{\text{match}}(y_i, \hat{y}_{\sigma(i)}), \quad (1)$$

with index $\sigma(i)$ and pair-wise costs C_{match} between ground truth y_i and prediction \hat{y}_i . The problem is solved with a combinatorial optimization algorithm as in [48]. Given the ground truth class labels c_i and predicted class probabilities $\hat{p}_i(c_i)$ for output embeddings i , the matching cost C_{match} with class weighting λ_{cls} is defined as

$$C_{\text{match}} = -\lambda_{\text{cls}} \hat{p}_{\sigma(i)}(c_i) + C_{\text{box}}(b_i, \hat{b}_{\sigma(i)}). \quad (2)$$

The authors of [7] report better performance without logarithmic class probabilities. The C_{box} term penalizes bounding box differences by a combination of ℓ_1 distance and generalized intersection over union (IoU) [40] cost C_{iou} ,

$$C_{\text{box}} = \lambda_{\ell_1} \|b_i - \hat{b}_{\sigma(i)}\|_1 + \lambda_{\text{iou}} C_{\text{iou}}(b_i, \hat{b}_{\sigma(i)}), \quad (3)$$

with weighting parameters $\lambda_{\ell_1}, \lambda_{\text{iou}} \in \mathfrak{R}$. In contrast to ℓ_1 , the scale-invariant IoU term provides similar relative errors for different box sizes. The optimal cost mapping $\hat{\sigma}$ determines the corresponding assignments in $\pi(i)$.

Set prediction loss. The final MOT set prediction loss is computed over all $N = N_{\text{object}} + N_{\text{track}}$ output predictions:

$$\mathcal{L}_{\text{MOT}}(y, \hat{y}, \pi) = \sum_{i=1}^N \mathcal{L}_{\text{query}}(y, \hat{y}_i, \pi). \quad (4)$$

The output embeddings which were not matched via track identity or $\hat{\sigma}$ are not part of the mapping π and will be assigned to the background class $c_i = 0$. We indicate the

ground truth object matched with prediction i by $y_{\pi=i}$ and define the loss per query

$$\mathcal{L}_{\text{query}} = \begin{cases} -\lambda_{\text{cls}} \log \hat{p}_i(c_{\pi=i}) + \mathcal{L}_{\text{box}}(b_{\pi=i}, \hat{b}_i), & \text{if } i \in \pi \\ -\lambda_{\text{cls}} \log \hat{p}_i(0), & \text{if } i \notin \pi. \end{cases}$$

The bounding box loss \mathcal{L}_{box} is computed in the same fashion as (3), but we differentiate its notation as the cost term C_{box} is generally not required to be differentiable.

Track augmentations. The two-step loss computation, see (i) and (ii), for training track queries represents only a limited range of possible tracking scenarios. Therefore, we propose the following augmentations to enrich the set of potential track queries during training. These augmentations will be verified in our experiments. We use three types of augmentations similar to [69] which lead to perturbations of object location and motion, missing detections, and simulated occlusions.

1. The frame $t - 1$ for step (i) is sampled from a range of frames around frame t , thereby generating challenging frame pairs where the objects have moved substantially from their previous position. Such a sampling allows for the simulation of camera motion and low frame rates from usually benevolent sequences.
2. We sample false negatives with a probability of p_{FN} by removing track queries before proceeding with step (ii). The corresponding ground truth objects in frame t will be matched with object queries and trigger a new object detection. Keeping the ratio of false positives sufficiently high is vital for a joined training of both query types.
3. To improve the removal of tracks, *i.e.*, by background class assignment, in occlusion scenarios, we complement the set of track queries with additional false positives. These queries are sampled from output embeddings of frame $t - 1$ that were classified as background. Each of the original track queries has a chance of p_{FP} to spawn an additional false positive query. We chose these with a large likelihood of occluding with the respective spawning track query.

Another common augmentation for improved robustness, is to applying spatial jittering to previous frame bounding boxes or center points [69]. The nature of track queries, which encode object information implicitly, does not allow for such an explicit perturbation in the spatial domain. We believe our randomization of the temporal range provides a more natural augmentation from video data.

4. Experiments

In this section, we present tracking results for TrackFormer on two MOTChallenge benchmarks, namely, MOT17 [30] and MOTS20 [52]. Furthermore, we verify individual contributions in an ablation study.

4.1. MOT benchmarks and metrics

Benchmarks. MOT17 [30] consists of a train and test set, each with 7 sequences and persons annotated with full-body bounding boxes. To evaluate only tracking, the public detection setting provides DPM [16], Faster R-CNN [39] and SDP [61] detections varying in quality.

The MOT20 [13] benchmark follows MOT17 but provides 4 train and 4 test sequences with crowded scenarios.

MOTS20 [52] provides mask annotations for 4 train and test sequences of MOT17 but without annotations for small objects. The corresponding bounding boxes are not full-body, but based on the visible segmentation masks.

Metrics. Different aspects of MOT are evaluated by a number of individual metrics [5]. The community focuses on Multiple Object Tracking Accuracy (MOTA) and Identity F1 Score (IDF1) [41]. While the former focuses on object coverage, the identity preservation is measured by the latter. For MOTS, we report MOTSA which evaluates predictions with a ground truth matching based on mask IoU.

Public detections. The MOT17 [30] benchmark is evaluated in a private and public detection setting. The latter allows for a comparison of tracking methods independent of the underlying object detection performance. MOT17 provides three sets of public detections with varying quality. In contrast to classic tracking-by-detection methods, TrackFormer is not able to directly produce tracking outputs from detection inputs. Therefore, we report the results of TrackFormer and CenterTrack [69] in Table 1 by filtering the initialization of tracks with a minimum IoU requirement. For more implementation details and a discussion on the fairness of such a filtering, we refer to the appendix.

4.2. Implementation details

TrackFormer follows the ResNet50 [18] CNN feature extraction and Transformer encoder-decoder architecture presented in Deformable DETR [71]. For track queries, the deformable reference points for the current frame are dynamically adjusted to the previous frame bounding box centers. Furthermore, for the decoder we stack the feature maps of the previous and current frame and compute cross-attention with queries over both frames. Queries are able to discriminate between features from the two frames by applying a temporal feature encoding as in [56]. For more detailed hyperparameters, we refer to the appendix.

Decoder Queries. By design, TrackFormer can only detect a maximum of N_{object} objects. To detect the maximum number of 52 objects per frame in MOT17 [30], we train TrackFormer with $N_{\text{object}} = 500$ learned object queries. For optimal performance, the total number of queries must exceed the number of ground truth objects per frame by a large margin. The number of possible track queries is adaptive and only practically limited by the abilities of the decoder.

Simulate MOT from single images. The encoder-decoder multi-level attention mechanism requires substantial amounts of training data. Hence, we follow a similar approach as in [69] and simulate MOT data from the CrowdHuman [45] person detection dataset. The adjacent training frames $t - 1$ and t are generated by applying random spatial augmentations to a single image. To generate challenging tracking scenarios, we randomly resize and crop of up to 20% with respect to the original image size.

Training procedure. All trainings follow [71] and apply a batch size of 2 with initial learning rates of 0.0002 and 0.00002 for the encoder-decoder and backbone, respectively. For public detections, we initialize with the model weights from [71] pretrained on COCO [28] and then fine-tune on MOT17 for 50 epochs with a learning rate drop after 10 epochs. The private detections model is trained from scratch for 85 epochs on CrowdHuman [45] with simulated adjacent frames and we drop the initial learning rates after 50 epochs. To avoid overfitting to the small MOT17 dataset, we then fine-tune for additional 40 epochs on the combined CrowdHuman and MOT17 datasets. The fine-tuning starts with the initial learning rates which are dropped after 10 epochs. By the nature of track queries each sample has a different number of total queries $N = N_{\text{object}} + N_{\text{track}}$. In order to stack samples to a batch, we pad the samples with additional false positive queries. The training of the private detections model takes around 2 days on $7 \times 32\text{GB}$ GPUs.

Mask training. TrackFormer predicts instance-level object masks with a segmentation head as in [7] by generating spatial attention maps from the encoded image features and decoder output embeddings. Subsequent upscaling and convolution operations yield mask predictions for all output embeddings. We adopt the private detection training pipeline from MOT17 but retrain TrackFormer with the original DETR [7] attention. This is due to the reduced memory consumption for single scale feature maps and inferior segmentation masks from sparse deformable attention maps. Furthermore, the benefits of deformable attention vanish on MOTS20 as it excludes small objects. After training on MOT17, we freeze the model and only train the segmentation head on all COCO images containing persons. Finally, we fine-tune the entire model on MOTS20.

Method	Data	FPS \uparrow	MOTA \uparrow	IDF1 \uparrow	MT \uparrow	ML \downarrow	FP \downarrow	FN \downarrow	ID Sw. \downarrow	
MOT17 [30] - Public										
Offline	jCC [22]	-	51.2	54.5	493	872	25937	247822	1802	
	FWT [19]	-	51.3	47.6	505	830	24101	247921	2648	
	eHAF [46]	-	51.8	54.7	551	893	33212	236772	1834	
	TT [65]	-	54.9	63.1	575	897	20236	233295	1088	
	MPNTrack [6]	M+C	-	58.8	61.7	679	788	17413	213594	1185
	Lif.T [20]	M+C	-	60.5	65.6	637	791	14966	206619	1189
Online	FAMNet [10]	-	52.0	48.7	450	787	14138	253616	3072	
	Tracktor++ [4]	M+C	1.3	56.3	55.1	498	831	8866	235449	1987
	GSM [29]	M+C	-	56.4	57.8	523	813	14379	230174	1485
	CenterTrack [69]	-	17.7	60.5	55.7	580	777	11599	208577	2540
	TMOH [47]	-	-	62.1	62.8	633	739	10951	201195	1897
	TrackFormer	-	7.4	62.3	57.6	688	638	16591	192123	4018
	MOT17 [30] - Private									
Online	TubeTK [32]	JTA	-	63.0	58.6	735	468	27060	177483	4137
	GSDT [55]	6M	-	73.2	66.5	981	411	26397	120666	3891
	FairMOT [66]	CH+6M	-	73.7	72.3	1017	408	27507	117477	3303
	PermaTrack [50]	CH+PD	-	73.8	68.9	1032	405	28998	115104	3699
	GRTU [54]	CH+6M	-	75.5	76.9	1158	495	27813	108690	1572
	TLR [53]	CH+6M	-	76.5	73.6	1122	300	29808	99510	3369
	CTracker [36]	-	-	66.6	57.4	759	570	22284	160491	5529
	CenterTrack [69]	CH	17.7	67.8	64.7	816	579	18498	160332	3039
	QuasiDense [33]	-	-	68.7	66.3	957	516	26589	146643	3378
	TraDeS [57]	CH	-	69.1	63.9	858	507	20892	150060	3555
	TrackFormer	CH	7.4	74.1	68.0	1113	246	34602	108777	2829
	MOT20 [13] - Private									
	Online	FairMOT [66]	CH+6M	-	61.8	67.3	855	94	103440	88901
GSDT [55]		6M	-	67.1	67.5	660	164	31913	135409	3131
SOTMOT [68]		CH+6M	-	68.6	71.4	806	120	57064	101154	4209
ReMOT [60]		CH+6M	-	77.4	73.1	846	123	28351	86659	1789
TrackFormer		CH	7.4	68.6	65.7	666	181	20348	140373	1532

Table 1. Comparison of multi-object tracking methods on the **MOT17** [30] and **MOT20** [13] test sets. We report private as well as public detection results and separate between online and offline approaches. Both TrackFormer and CenterTrack filter tracks by requiring a minimum IoU with public detections. For a detailed discussion on the fairness of such a filtering, we refer to the appendix. We indicated additional training *Data*: CH= CrowdHuman [45], PD=Parallel Domain [50], 6M=6 tracking datasets as in [66], JTA [14], M=Market1501 [67] and C=CUHK03 [27]. Runtimes (FPS) are self-measured.

4.3. Benchmark results

MOT17. Following the training procedure described in Section 4.2, we evaluate TrackFormer on the MOT17 [30] test set and report results in Table 1.

First of all, we isolate the tracking performance and compare results in a public detection setting by applying a track initialization filtering similar to [69]. However to improve fairness, we filter not by bounding box center distance as in [69] but a minimum IoU as detailed in the appendix. TrackFormer performs on-par with state-of-the-art results in terms of MOTA without pretraining on CrowdHuman [45]. Our identity preservation performance is only surpassed by [47] and offline methods which benefit from the processing of entire sequences at once.

On private detections, we achieve a new state-of-the-art both in terms of MOTA (+5.0) and IDF1 (1.7) for methods only trained on CrowdHuman [45]. Only [50, 53, 54] which

follow [66] and pretrain on 6 additional tracking datasets (6M) surpass our performance. In contrast to our public detection model not only the detection but tracking performance are greatly improved. This is due to the additional tracking data required by Transformers and provided via adjacent frame simulation on CrowdHuman.

MOT20. On MOT20 [13], we introduce the first method only pretrained on CrowdHuman [45] (CH). However, we surpass or perform on-par with several modern methods [55, 66, 68] that were trained on significantly more data, *i.e.*, 6 additional tracking datasets (6M).

Our tracking-by-attention approach achieves top performance via global attention without relying on additional motion [4, 10] or appearance models [4, 8, 10]. Furthermore, the frame association with track queries avoids post-processing with heuristic greedy matching procedures [69] or additional graph optimization [29]. Our proposed TrackFormer represents the first application of Transformers to the MOT problem and could work as a blueprint for future research. In particular, we expect great potential for methods going beyond our two-frame training/inference.

MOTS20. In addition to detection and tracking, TrackFormer is able to predict instance-level segmentation masks. As reported in Table 2, we achieve state-of-the-art object coverage (MOTSA) and identity preservation (IDF1) results for MOTS. All methods are evaluated in a private setting. A MOTS20 [52] test set submission is only recently possible, hence we also provide the 4-fold cross-validation evaluation established in [52] reporting the mean best epoch results. TrackFormer surpasses all previous methods without relying on a dedicated mask tracking formulation as in [58]. In Figure 3, we qualitatively compare TrackFormer and Track R-CNN [52] on two test sequences.

4.4. Ablation study

The ablation study on the MOT17 and MOTS20 training sequences are evaluated in a private detection setting with a 50-50 frame and 4-fold cross-validation split, respectively.

TrackFormer components. We ablate the impact of different TrackFormer components on the tracking performance in Table 3. Our full pipeline including pretraining on the CrowdHuman dataset provides a MOTA and IDF1 of 71.3 and 73.4, respectively. The baseline without (w/o) pretraining reduces this by -2.0 and -1.6 points, an effect expected to even more severe for the generalization to test. The attention-based *track query re-identification* has a negligible effect on MOTA but improves IDF1 by 1.4 points.

The ablation of false positive (FP) and frame range *track augmentations* yields another drop of -5.2 MOTA and -11.2

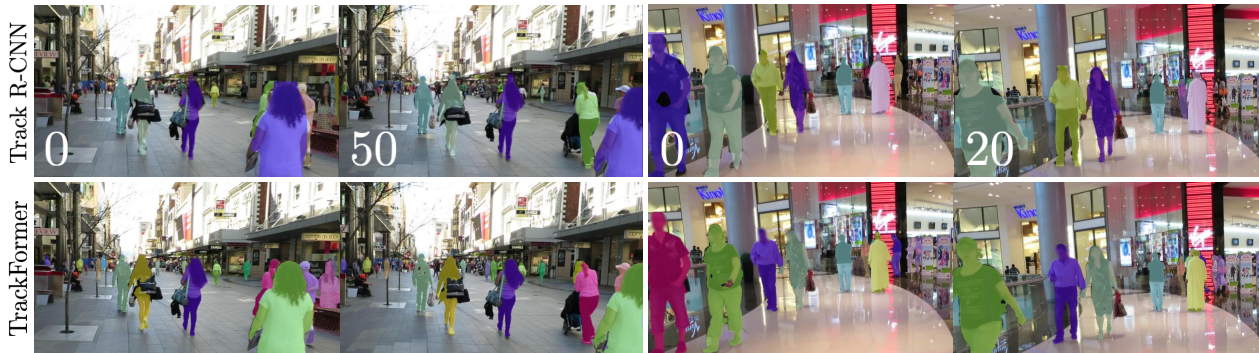


Figure 3. We compare **TrackFormer segmentation results** with the popular Track R-CNN [52] on selected MOTS20 [52] test sequences. The superiority of TrackFormer in terms of MOTSA in Table 2 can be clearly observed by the difference in pixel mask accuracy.

Method	TbD	sMOTSA \uparrow	IDF1 \uparrow	FP \downarrow	FN \downarrow	ID Sw. \downarrow
Train set (4-fold cross-validation)						
MHT_DAM [23]	×	48.0	-	-	-	-
FWT [19]	×	49.3	-	-	-	-
MOTDT [8]	×	47.8	-	-	-	-
jCC [22]	×	48.3	-	-	-	-
TrackRCNN [52]		52.7	-	-	-	-
MOTNet [38]		56.8	-	-	-	-
PointTrack [58]		58.1	-	-	-	-
TrackFormer		58.7	-	-	-	-
Test set						
Track R-CNN [52]		40.6	42.4	1261	12641	567
TrackFormer		54.9	63.6	2233	7195	278

Table 2. Comparison of multi-object tracking and segmentation methods evaluated on the MOTS20 [52] train and test sets. We indicate methods which first perform tracking-by-detection (TbD) on SDP [62] detections and then apply a Mask R-CNN [17].

Method	MOTA \uparrow	Δ	IDF1 \uparrow	Δ
TrackFormer	71.3		73.4	
— w/o —				
Pretraining on CrowdHuman	69.3	-2.0	71.8	-1.6
Track query re-identification	69.2	-0.1	70.4	-1.4
Track augmentations (FP)	68.4	-0.8	70.0	-0.4
Track augmentations (Range)	64.0	-4.4	59.2	-10.8
Track queries	61.0	-3.0	45.1	-14.1

Table 3. **Ablation study** on TrackFormer components. We report MOT17 [30] training set private results on a 50-50 frame split. The last row without (w/o) all components is only trained for object detection and associates tracks via greedy matching as in [69].

IDF1 points. Both augment the training with rich tracking scenarios preventing an early overfitting. The false negative augmentations are indispensable for a joint training of object and track queries, hence we refrain from ablating these.

The last row also removes *track queries* and is only trained for object detection. Tracks are associated via

Method	Mask training	MOTA \uparrow	IDF1 \uparrow
TrackFormer	×	61.9	56.0
		61.9	54.8

Table 4. We demonstrate the **effect of jointly training for tracking and segmentation** on a 4-fold split on the MOTS20 [52] train set. We evaluate with regular MOT metrics, *i.e.*, matching to ground truth with bounding boxes instead of masks.

greedy center distance matching as in [69] resulting in a huge drop of -3.0 MOTA and -14.1 IDF1. This version represents previous heuristic matching methods and demonstrates the benefit of jointly addressing track initialization and association in a unified TrackFormer formulation.

Mask information improves tracking. This ablation studies the synergies between segmentation and tracking training. Table 4 only evaluates bounding box tracking performance and shows a +1.2 IDF1 improvement when trained jointly with mask prediction. The additional mask information does not improve track coverage (MOTA) but resolves ambiguous occlusion scenarios during training.

5. Conclusion

We have presented a unified tracking-by-attention paradigm for detection and multi-object tracking with Transformers. As an example of said paradigm, our end-to-end trainable TrackFormer architecture applies autoregressive track query embeddings to follow objects over a sequence. We jointly tackle track initialization, identity and trajectory forming with a Transformer encoder-decoder architecture and not relying on additional matching, graph optimization or motion/appearance modeling. Our approach achieves state-of-the-art results for multi-object tracking as well as segmentation. We hope that this paradigm will foster future work in Transformers for multi-object tracking.

Acknowledgements: We are grateful for discussions with Jitendra Malik, Karttikeya Mangalam, and David Novotny.

Appendix

This section provides additional material for the main paper: §A contains further implementation details for TrackFormer (§A.1), a visualization of the Transformer encoder-decoder architecture (§A.3), and parameters for multi-object tracking (§A.4). §B contains a discussion related to public detection evaluation (§B.1), and detailed per-sequence results for MOT17 and MOTS20 (§B.2).

A. Implementation details

A.1. Backbone and training

We provide additional hyperparameters for TrackFormer. This supports our implementation details reported in Section 4.2 of the main paper. The Deformable DETR [71] encoder and decoder both apply 6 individual layers with multi-headed self-attention [51] with 8 attention heads. We do not use the “DC5” (dilated conv₅) version of the backbone as this will incur a large memory requirement related to the larger resolution of the last residual stage. We expect that using “DC5” or any other heavier, or higher-resolution, backbone to provide better accuracy and leave this for future work. Furthermore, we also apply the refinement of deformable reference point coined as *bounding box refinement* in [71].

Our training hyperparameters follow deformable DETR [71]. The weighting parameters of the cost and their corresponding loss terms are set to $\lambda_{\text{cls}} = 2$, $\lambda_{\ell_1} = 5$ and $\lambda_{\text{iou}} = 2$. The probabilities for the track augmentation at training time are $p_{\text{FN}} = 0.4$ and $p_{\text{FP}} = 0.1$. Furthermore, every MOT17 [30] frame is jittered by 1% with respect to the original image size similar to the adjacent frame simulation.

A.2. Dataset splits

All experiments evaluated on dataset splits (ablation studies and MOTS20 training set in Table 2) apply the same private training pipeline presented in Section 4.2 to each split. For our ablation on the MOT17 [30] training set, we separate the 7 sequences into 2 splits and report results from training on the first 50% and evaluating on the last 50% of frames. For MOTS20 we average validation metrics over all splits and report the results from a single epoch (which yields the best mean MOTA / MOTSA) over all splits, *i.e.*, we do not take the best epoch for each individual split. Before training each of the 4 MOTS20 [52] splits, we pre-train the model on all MOT17 sequences excluding the corresponding split of the validation sequence.

A.3. Transformer encoder-decoder architecture

To foster the understanding of TrackFormer’s integration of track queries within the decoder self-attention block, we provide a simplified visualization of the encoder-decoder architecture in Figure A.1. In comparison to the original illustration in [7], we indicate *track identities* instead of spatial encoding with *color-coded* queries. The frame features (indicated in grey) are the final output of the CNN feature extractor and have the same number of channels as both query types. The entire Transformer architecture applies $N = 6$ and $M = 6$ independently supervised encoder and decoder layers, with feature and object encoding as in [7]. To improve, tracking consistency we stack the feature maps of the previous and current frame and apply a spatial positional and temporal encoding as in [56]. Track queries are fed *autoregressively* from the *previous frame* output embeddings of the last decoding layer (before the final feed-forward class and bounding box networks (FFN)). The object encoding is achieved by adding the initial object queries to the key (K) and query (Q) of the corresponding embeddings at each decoder layer.

A.4. Multi-object tracking parameters

In Section 3.2 , we explain the process of track initialization and removal over a sequence. The corresponding hyperparameters were optimized by a grid search on the MOT17 validation split. The grid search yielded track initialization and removal thresholds of $\sigma_{\text{detection}} = 0.4$ and $\sigma_{\text{track}} = 0.4$, respectively. TrackFormer benefits from an NMS operation for the removal of strong occlusion cases with an intersection over union larger than $\sigma_{\text{NMS}} = 0.9$.

For the track query re-identification, our search proposed an optimal inactive patience and score of $T_{\text{track-reid}} = 5$ and $\sigma_{\text{track-reid}} = 0.4$, respectively.

B. Experiments

B.1. Public detections and track filtering

TrackFormer implements a new tracking-by-attention paradigm which requires track initializations to be filtered for an evaluation with public detections. Here, we provide a discussion on the comparability of TrackFormer with earlier methods and different filtering schemes.

Common tracking-by-detection methods directly process the MOT17 public detections and report their mean tracking performance over all three sets. This is only possible for methods that perform data association on a bounding box level. However, TrackFormer and point-based methods such as CenterTrack [69] require a procedure for filtering track initializations by public detections in a comparable manner. Unfortunately, MOT17 does not provide a standardized protocol for such a filtering. The authors of CenterTrack [69] filter detections based on bounding box center

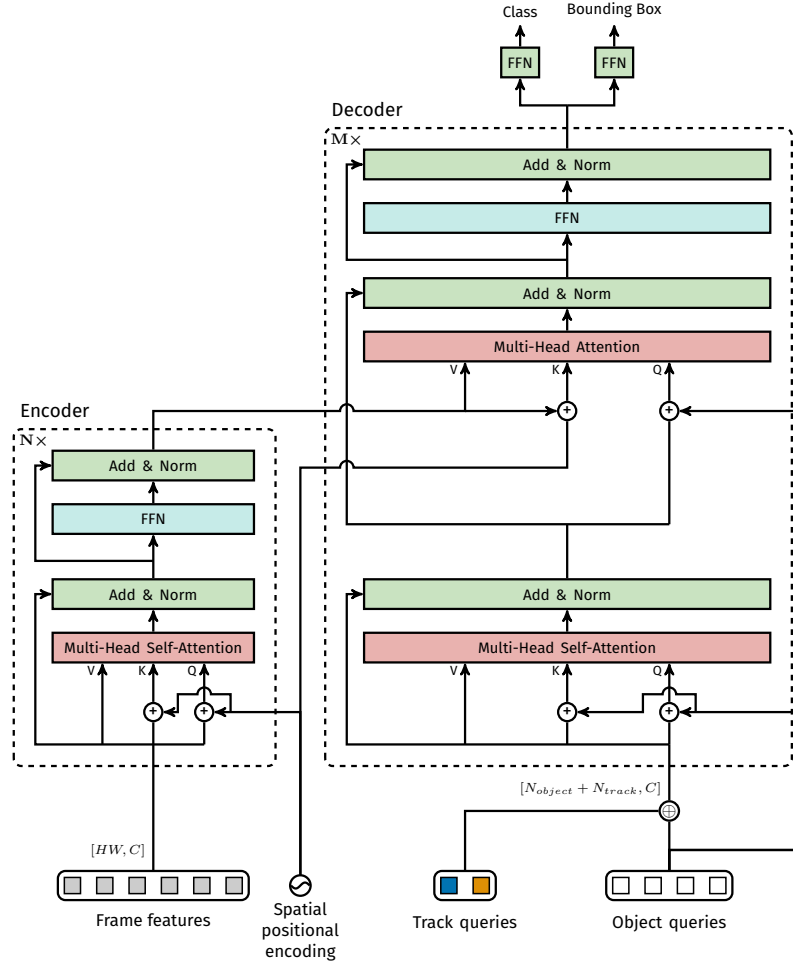


Figure A.1. The TrackFormer encoder-decoder architecture. We indicate the tensor dimensions in squared brackets.

distances (CD). Each public detection can possibly initialize a single track but only if its center point falls in the bounding box area of the corresponding track.

In Table A.1, we revisit our MOT17 test set results but with this public detections center distance (CD) filtering, while also inspecting the CenterTrack per-sequence results in Table A.6. We observe that this filtering does not reflect the quality differences in each set of public detections, *i.e.*, DPM [16] and SDP [61] results are expected to be the worst and best, respectively, but their difference is small.

We hypothesize that a center distance filtering is not in accordance with the common public detection setting and propose a filtering based on Intersection over Union (IoU). For IoU filtering, public detections only initialize a track if they have an IoU larger than 0.5. The results in Table A.1 show that for TrackFormer and CenterTrack IoU filtering performs worse compared to the CD filtering which is expected as this is a more challenging evaluation protocol. We believe IoU-based filtering (instead of CD-based) provides

a fairer comparison to previous MOT methods which directly process public detections as inputs (IN). This is validated by the per-sequence results in Table A.3, where IoU filtering shows differences across detectors that are more meaningfully correlated with detector performance, compared to the relatively uniform performance across detections with the CD based method in Table A.6 (where DPM, FRCNN and SDP show *very similar* performance).

Consequently, we follow the IoU-based filtering protocol to compare with CenterTrack in our main paper. While our gain over CenterTrack seems similar across the two filtering techniques for MOTA (see Table A.1), the gain in IDF1 is significantly larger under the more challenging IoU-based protocol, which suggests that CenterTrack benefits from the less challenging CD-based filtering protocol, while TrackFormer does not rely on the filtering for achieving its high IDF1 tracking accuracy.

Method	IN	IoU	CD	MOTA \uparrow	IDF1 \uparrow
Offline					
MHT_DAM [23]	×			50.7	47.2
jCC [22]	×			51.2	54.5
FWT [19]	×			51.3	47.6
eHAF [46]	×			51.8	54.7
TT [65]	×			54.9	63.1
MPNTrack [6]	×			58.8	61.7
Lif_T [20]	×			60.5	65.6
Online					
MOTDT [8]	×			50.9	52.7
FAMNet [10]	×			52.0	48.7
Tracktor++ [4]	×			56.3	55.1
GSM_Tracktor [29]	×			56.4	57.8
TMOH [47]	×			62.1	62.8
CenterTrack [69]		×		60.5	55.7
TrackFormer		×		62.3	57.6
CenterTrack [69]			×	61.5	59.6
TrackFormer			×	63.4	60.0

Table A.1. Comparison of modern multi-object tracking methods evaluated on the **MOT17** [30] test set for different **public detection processing**. Public detections are either directly processed as input (IN) or applied for filtering of track initializations by center distance (CD) or intersection over union (IoU). We report mean results over the three sets of public detections provided by [30] and separate between online and offline approaches. The arrows indicate low or high optimal metric values.

B.2. MOT17, MOT20 and MOTS20 results

In Table A.2 and and Table A.3, we provide per-sequence MOT17 [30] test set results for private and public detection filtering via Intersection over Union (IoU), respectively.

For per-sequence results on MOT20, we refer to Table A.4. Furthermore, we present per-sequence TrackFormer results on the MOTS20 [52] test set in Table A.5.

Evaluation metrics In Section 4.1 we explained two compound metrics for the evaluation of MOT results, namely, Multi-Object Tracking Accuracy (MOTA) and Identity F1 score (IDF1). However, the **MOTChallenge** benchmark implements all CLEAR MOT [5] evaluation metrics. In addition to MOTA and IDF1, we report the following CLEAR MOT metrics:

MT: Ground truth tracks covered for at least 80%.

ML: Ground truth tracks covered for at most 20%.

FP: False positive bounding boxes not corresponding to any ground truth.

FN: False negative ground truth boxes not covered by any bounding box.

ID Sw.: Bounding boxes switching the corresponding ground truth identity.

sMOTSA: Mask-based Multi-Object Tracking Accuracy (MOTA) which counts true positives instead of only masks with IoU larger than 0.5.

Sequence	Public detection	MOTA \uparrow	IDF1 \uparrow	MT \uparrow	ML \downarrow	FP \downarrow	FN \downarrow	ID Sw. \downarrow
MOT17-01	DPM [16]	57.9	49.7	11	4	477	2191	45
MOT17-03	DPM	88.6	79.6	124	3	2469	9365	122
MOT17-06	DPM	59.8	60.8	104	27	1791	2775	173
MOT17-07	DPM	65.5	49.5	24	5	1030	4671	118
MOT17-08	DPM	54.5	42.5	24	9	1461	7861	279
MOT17-12	DPM	51.8	63.0	43	14	1880	2258	42
MOT17-14	DPM	47.4	54.9	41	20	2426	7138	164
MOT17-01	FRCNN [39]	57.9	49.7	11	4	477	2191	45
MOT17-03	FRCNN	88.6	79.6	124	3	2469	9365	122
MOT17-06	FRCNN	59.8	60.8	104	27	1791	2775	173
MOT17-07	FRCNN	65.5	49.5	24	5	1030	4671	118
MOT17-08	FRCNN	54.5	42.5	24	9	1461	7861	279
MOT17-12	FRCNN	51.8	63.0	43	14	1880	2258	42
MOT17-14	FRCNN	47.4	54.9	41	20	2426	7138	164
MOT17-01	SDP [61]	57.9	49.7	11	4	477	2191	45
MOT17-03	SDP	88.6	79.6	124	3	2469	9365	122
MOT17-06	SDP	59.8	60.8	104	27	1791	2775	173
MOT17-07	SDP	65.5	49.5	24	5	1030	4671	118
MOT17-08	SDP	54.5	42.5	24	9	1461	7861	279
MOT17-12	SDP	51.8	63.0	43	14	1880	2258	42
MOT17-14	SDP	47.4	54.9	41	20	2426	7138	164
All	All	74.1	68.0	1113	246	34602	108777	2829

Table A.2. We report **private TrackFormer** results on each individual sequence evaluated on the **MOT17** [30] test set. To follow the official MOT17 format, we display the same results per public detection set. The arrows indicate low or high optimal metric values.

Sequence	Public detection	MOTA \uparrow	IDF1 \uparrow	MT \uparrow	ML \downarrow	FP \downarrow	FN \downarrow	ID Sw. \downarrow
MOT17-01	DPM [16]	49.9	43.0	5	8	258	2932	40
MOT17-03	DPM	74.0	66.5	85	18	1389	25396	374
MOT17-06	DPM	53.6	51.8	63	75	711	4575	180
MOT17-07	DPM	52.6	48.1	12	16	258	7663	88
MOT17-08	DPM	32.5	31.9	10	32	288	13838	128
MOT17-12	DPM	51.3	57.7	21	31	606	3565	53
MOT17-14	DPM	38.1	42.0	15	63	627	10505	314
MOT17-01	FRCNN [39]	50.9	42.3	8	6	308	2813	48
MOT17-03	FRCNN	75.3	67.0	84	16	1434	24040	335
MOT17-06	FRCNN	57.2	54.8	73	48	960	3856	226
MOT17-07	FRCNN	52.4	47.9	12	11	499	7437	106
MOT17-08	FRCNN	31.1	31.7	10	36	285	14166	102
MOT17-12	FRCNN	47.7	56.7	19	32	702	3785	45
MOT17-14	FRCNN	37.8	41.8	17	56	1300	9795	406
MOT17-01	SDP [61]	53.7	45.3	10	5	556	2386	47
MOT17-03	SDP	79.6	65.8	95	13	2134	18632	545
MOT17-06	SDP	56.4	54.0	82	57	1017	3889	228
MOT17-07	SDP	54.6	47.8	16	11	590	6965	121
MOT17-08	SDP	35.0	33.0	12	27	443	13152	144
MOT17-12	SDP	48.9	57.5	22	28	850	3527	54
MOT17-14	SDP	40.4	42.4	17	49	1376	9206	434
ALL	ALL	62.3	57.6	688	638	16591	192123	4018

Table A.3. We report **TrackFormer** results on each individual sequence and set of public detections evaluated on the **MOT17** [30] test set. We apply our minimum **Intersection over Union (IoU)** public detection filtering. The arrows indicate low or high optimal metric values.

Sequence	MOTA \uparrow	IDF1 \uparrow	MT \uparrow	ML \downarrow	FP \downarrow	FN \downarrow	ID Sw. \downarrow
MOT20-04	82.7	75.6	490	28	9639	37165	566
MOT20-06	55.9	53.5	96	72	5582	52440	545
MOT20-07	56.2	59.0	41	20	547	13856	92
MOT20-08	46.0	48.3	39	61	4580	36912	329
ALL	68.6	65.7	666	181	20348	140373	1532

Table A.4. We report **private TrackFormer** results on each individual sequence evaluated on the **MOT20** [13] test set. The arrows indicate low or high optimal metric values.

Sequence	sMOTSA \uparrow	IDF1 \uparrow	MOTSA \uparrow	FP \downarrow	FN \downarrow	ID Sw. \downarrow
MOTS20-01	59.8	68.0	79.6	255	364	16
MOTS20-06	63.9	65.1	78.7	595	1335	158
MOTS20-07	43.2	53.6	58.5	834	4433	75
MOTS20-12	62.0	76.8	74.6	549	1063	29
ALL	54.9	63.6	69.9	2233	7195	278

Table A.5. We present TrackFormer tracking and segmentation results on each individual sequence of the **MOTS20** [52] test set. MOTS20 is evaluated in a private detections setting. The arrows indicate low or high optimal metric values.

Sequence	Public detection	MOTA \uparrow	IDF1 \uparrow	MT \uparrow	ML \downarrow	FP \downarrow	FN \downarrow	ID Sw. \downarrow
MOT17-01	DPM [16]	41.6	44.2	5	8	496	3252	22
MOT17-03	DPM	79.3	71.6	94	8	1142	20297	191
MOT17-06	DPM	54.8	42.0	54	63	314	4839	175
MOT17-07	DPM	44.8	42.0	11	16	1322	7851	147
MOT17-08	DPM	26.5	32.2	11	37	378	15066	88
MOT17-12	DPM	46.1	53.1	16	45	207	4434	30
MOT17-14	DPM	31.6	36.6	13	78	636	11812	196
MOT17-01	FRCNN [39]	41.0	42.1	6	9	571	3207	25
MOT17-03	FRCNN	79.6	72.7	93	7	1234	19945	180
MOT17-06	FRCNN	55.6	42.9	57	59	363	4676	190
MOT17-07	FRCNN	45.5	41.5	13	15	1263	7785	156
MOT17-08	FRCNN	26.5	31.9	11	36	332	15113	89
MOT17-12	FRCNN	46.1	52.6	15	45	197	4443	30
MOT17-14	FRCNN	31.6	37.6	13	77	780	11653	202
MOT17-01	SDP [61]	41.8	44.3	7	8	612	3112	27
MOT17-03	SDP	80.0	72.0	93	8	1223	19530	181
MOT17-06	SDP	55.5	43.8	56	61	354	4712	181
MOT17-07	SDP	45.2	42.4	13	15	1332	7775	147
MOT17-08	SDP	26.6	32.3	11	36	350	15067	91
MOT17-12	SDP	46.0	53.0	16	45	221	4426	30
MOT17-14	SDP	31.7	37.1	13	76	749	11677	205
All	All	61.5	59.6	621	752	14076	200672	2583

Table A.6. We report the original per-sequence **CenterTrack** [69] **MOT17** [30] test set results with **Center Distance (CD)** public detection filtering. The results do not reflect the varying object detection performance of DPM, FRCNN and SDP, respectively. The arrows indicate low or high optimal metric values.

References

- [1] Alexandre Alahi, Kratharth Goel, Vignesh Ramanathan, Alexandre Robicquet, Li Fei-Fei, and Silvio Savarese. Social lstm: Human trajectory prediction in crowded spaces. *IEEE Conf. Comput. Vis. Pattern Recog.*, 2016. [2](#)
- [2] Anton Andriyenko and Konrad Schindler. Multi-target tracking by continuous energy minimization. *IEEE Conf. Comput. Vis. Pattern Recog.*, 2011. [2](#)
- [3] Jerome Berclaz, Francois Fleuret, Engin Turetken, and Pascal Fua. Multiple object tracking using k-shortest paths optimization. *IEEE Trans. Pattern Anal. Mach. Intell.*, 2011. [2](#)
- [4] Philipp Bergmann, Tim Meinhardt, and Laura Leal-Taixé. Tracking without bells and whistles. In *Int. Conf. Comput. Vis.*, 2019. [1](#), [2](#), [7](#), [11](#)
- [5] Keni Bernardin and Rainer Stiefelwagen. Evaluating multiple object tracking performance: the clear mot metrics. *EURASIP Journal on Image and Video Processing*, 2008, 2008. [6](#), [11](#)
- [6] Guillem Brasó and Laura Leal-Taixé. Learning a neural solver for multiple object tracking. In *IEEE Conf. Comput. Vis. Pattern Recog.*, 2020. [1](#), [2](#), [7](#), [11](#)
- [7] Nicolas Carion, F. Massa, Gabriel Synnaeve, Nicolas Usunier, Alexander Kirillov, and Sergey Zagoruyko. End-to-end object detection with transformers. *Eur. Conf. Comput. Vis.*, 2020. [1](#), [2](#), [3](#), [5](#), [6](#), [9](#)
- [8] Long Chen, Haizhou Ai, Zijie Zhuang, and Chong Shang. Real-time multiple people tracking with deeply learned candidate selection and person re-identification. In *Int. Conf. Multimedia and Expo*, 2018. [1](#), [2](#), [7](#), [8](#), [11](#)
- [9] Wongun Choi and Silvio Savarese. Multiple target tracking in world coordinate with single, minimally calibrated camera. *Eur. Conf. Comput. Vis.*, 2010. [2](#)
- [10] Peng Chu and Haibin Ling. Famnet: Joint learning of feature, affinity and multi-dimensional assignment for online multiple object tracking. In *Int. Conf. Comput. Vis.*, 2019. [2](#), [7](#), [11](#)
- [11] Qi Chu, Wanli Ouyang, Hongsheng Li, Xiaogang Wang, Bin Liu, and Nenghai Yu. Online multi-object tracking using cnn-based single object tracker with spatial-temporal attention mechanism. In *Proceedings of the IEEE International Conference on Computer Vision*, pages 4836–4845, 2017. [1](#), [2](#)
- [12] Patrick Dendorfer, Aljosa Osep, Anton Milan, Daniel Cremers, Ian Reid, Stefan Roth, and Laura Leal-Taixé. Motchallenge: A benchmark for single-camera multiple target tracking. *Int. J. Comput. Vis.*, 2020. [1](#)
- [13] Patrick Dendorfer, Hamid Rezatofighi, Anton Milan, Javen Shi, Daniel Cremers, Ian D. Reid, Stefan Roth, Konrad Schindler, and Laura Leal-Taixé. MOT20: A benchmark for multi object tracking in crowded scenes. *CoRR*, 2020. [2](#), [6](#), [7](#), [13](#)
- [14] Matteo Fabbri, Fabio Lanzi, Simone Calderara, Andrea Palazzi, Roberto Vezzani, and Rita Cucchiara. Learning to detect and track visible and occluded body joints in a virtual world. In *European Conference on Computer Vision (ECCV)*, 2018. [7](#)
- [15] Christoph Feichtenhofer, Axel Pinz, and Andrew Zisserman. Detect to track and track to detect. In *ICCV*, 2017. [2](#)
- [16] Pedro F. Felzenszwalb, Ross B. Girshick, David A. McAllester, and Deva Ramanan. Object detection with discriminatively trained part based models. *IEEE Trans. Pattern Anal. Mach. Intell.*, 2009. [6](#), [10](#), [12](#), [13](#)
- [17] Kaiming He, Georgia Gkioxari, Piotr Dollár, and Ross Girshick. Mask r-cnn. In *IEEE Conf. Comput. Vis. Pattern Recog.*, 2017. [2](#), [8](#)
- [18] Kaiming He, Xiangyu Zhang, Shaoqing Ren, and Jian Sun. Deep residual learning for image recognition. In *IEEE Conf. Comput. Vis. Pattern Recog.*, 2016. [2](#), [3](#), [6](#)
- [19] Roberto Henschel, Laura Leal-Taixé, Daniel Cremers, and Bodo Rosenhahn. Improvements to frank-wolfe optimization for multi-detector multi-object tracking. In *IEEE Conf. Comput. Vis. Pattern Recog.*, 2017. [1](#), [2](#), [7](#), [8](#), [11](#)
- [20] Andrea Hornakova, Roberto Henschel, Bodo Rosenhahn, and Paul Swoboda. Lifted disjoint paths with application in multiple object tracking. In *Int. Conf. Mach. Learn.*, 2020. [2](#), [7](#), [11](#)
- [21] Hao Jiang, Sidney S. Fels, and James J. Little. A linear programming approach for multiple object tracking. *IEEE Conf. Comput. Vis. Pattern Recog.*, 2007. [2](#)
- [22] Margret Keuper, Siyu Tang, Bjoern Andres, Thomas Brox, and Bernt Schiele. Motion segmentation & multiple object tracking by correlation co-clustering. In *IEEE Trans. Pattern Anal. Mach. Intell.*, 2018. [1](#), [2](#), [7](#), [8](#), [11](#)
- [23] Chanh Kim, Fuxin Li, Arridhana Ciptadi, and James M. Rehg. Multiple hypothesis tracking revisited. In *Int. Conf. Comput. Vis.*, 2015. [1](#), [2](#), [8](#), [11](#)
- [24] Laura Leal-Taixé, Cristian Canton-Ferrer, and Konrad Schindler. Learning by tracking: siamese cnn for robust target association. *IEEE Conf. Comput. Vis. Pattern Recog. Worksh.*, 2016. [1](#), [2](#)
- [25] Laura Leal-Taixé, Michele Fenzi, Alina Kuznetsova, Bodo Rosenhahn, and Silvio Savarese. Learning an image-based motion context for multiple people tracking. *IEEE Conf. Comput. Vis. Pattern Recog.*, 2014. [2](#)
- [26] Laura Leal-Taixé, Gerard Pons-Moll, and Bodo Rosenhahn. Everybody needs somebody: Modeling social and grouping behavior on a linear programming multiple people tracker. *Int. Conf. Comput. Vis. Workshops*, 2011. [1](#), [2](#)
- [27] Wei Li, Rui Zhao, Tong Xiao, and Xiaogang Wang. Deep-reid: Deep filter pairing neural network for person re-identification. In *IEEE Conf. Comput. Vis. Pattern Recog.*, 2014. [7](#)
- [28] Tsung-Yi Lin, Michael Maire, Serge Belongie, Lubomir Bourdev, Ross Girshick, James Hays, Pietro Perona, Deva Ramanan, C. Lawrence Zitnick, and Piotr Dollár. Microsoft coco: Common objects in context. *arXiv:1405.0312*, 2014. [6](#)
- [29] Qiankun Liu, Qi Chu, Bin Liu, and Nenghai Yu. Gsm: Graph similarity model for multi-object tracking. In *Int. Joint Conf. Art. Int.*, 2020. [1](#), [2](#), [7](#), [11](#)
- [30] Anton Milan, Laura Leal-Taixé, Ian D. Reid, Stefan Roth, and Konrad Schindler. Mot16: A benchmark for multi-object tracking. *arXiv:1603.00831*, 2016. [2](#), [6](#), [7](#), [8](#), [9](#), [11](#), [12](#), [13](#)

- [31] Aljoša Ošep, Wolfgang Mehner, Paul Voigtlaender, and Bastian Leibe. Track, then decide: Category-agnostic vision-based multi-object tracking. *IEEE Int. Conf. Rob. Aut.*, 2018. [2](#)
- [32] Bo Pang, Yizhuo Li, Yifan Zhang, Muchen Li, and Cewu Lu. Tubetk: Adopting tubes to track multi-object in a one-step training model. In *Proceedings of the IEEE/CVF Conference on Computer Vision and Pattern Recognition (CVPR)*, June 2020. [7](#)
- [33] Jiangmiao Pang, Linlu Qiu, Xia Li, Haofeng Chen, Qi Li, Trevor Darrell, and Fisher Yu. Quasi-dense similarity learning for multiple object tracking. In *IEEE/CVF Conference on Computer Vision and Pattern Recognition*, June 2021. [2](#), [7](#)
- [34] Niki Parmar, Ashish Vaswani, Jakob Uszkoreit, Łukasz Kaiser, Noam Shazeer, Alexander Ku, and Dustin Tran. Image transformer. *arXiv preprint arXiv:1802.05751*, 2018. [2](#)
- [35] Stefano Pellegrini, Andreas Ess, Konrad Schindler, and Luc Van Gool. You'll never walk alone: modeling social behavior for multi-target tracking. *Int. Conf. Comput. Vis.*, 2009. [2](#)
- [36] Jinlong Peng, Changan Wang, Fangbin Wan, Yang Wu, Yabiao Wang, Ying Tai, Chengjie Wang, Jilin Li, Feiyue Huang, and Yanwei Fu. Chained-tracker: Chaining paired attentive regression results for end-to-end joint multiple-object detection and tracking. In *Proceedings of the European Conference on Computer Vision*, 2020. [7](#)
- [37] Hamed Pirsiavash, Deva Ramanan, and Charless C. Fowlkes. Globally-optimal greedy algorithms for tracking a variable number of objects. *IEEE Conf. Comput. Vis. Pattern Recog.*, 2011. [2](#)
- [38] Lorenzo Porzi, Markus Hofinger, Idoia Ruiz, Joan Serrat, Samuel Rota Buló, and Peter Kotschieder. Learning multi-object tracking and segmentation from automatic annotations. In *IEEE Conf. Comput. Vis. Pattern Recog.*, 2020. [2](#), [8](#)
- [39] Shaoqing Ren, Kaiming He, Ross Girshick, and Jian Sun. Faster r-cnn: Towards real-time object detection with region proposal networks. *Adv. Neural Inform. Process. Syst.*, 2015. [1](#), [6](#), [12](#), [13](#)
- [40] Hamid Rezaatofghi, Nathan Tsoi, JunYoung Gwak, Amir Sadeghian, Ian Reid, and Silvio Savarese. Generalized intersection over union: A metric and a loss for bounding box regression. In *IEEE Conf. Comput. Vis. Pattern Recog.*, 2019. [5](#)
- [41] Ergys Ristani, Francesco Solera, Roger S. Zou, Rita Cucchiara, and Carlo Tomasi. Performance measures and a data set for multi-target, multi-camera tracking. In *Eur. Conf. Comput. Vis. Workshops*, 2016. [6](#)
- [42] Ergys Ristani and Carlo Tomasi. Features for multi-target multi-camera tracking and re-identification. *IEEE Conf. Comput. Vis. Pattern Recog.*, 2018. [2](#)
- [43] Alexandre Robicquet, Amir Sadeghian, Alexandre Alahi, and Silvio Savarese. Learning social etiquette: Human trajectory prediction. *Eur. Conf. Comput. Vis.*, 2016. [2](#)
- [44] Paul Scovanner and Marshall F. Tappen. Learning pedestrian dynamics from the real world. *Int. Conf. Comput. Vis.*, 2009. [2](#)
- [45] Shuai Shao, Zijian Zhao, Boxun Li, Tete Xiao, Gang Yu, Xiangyu Zhang, and Jian Sun. Crowdhuman: A benchmark for detecting human in a crowd. *arXiv:1805.00123*, 2018. [6](#), [7](#)
- [46] H. Sheng, Y. Zhang, J. Chen, Z. Xiong, and J. Zhang. Heterogeneous association graph fusion for target association in multiple object tracking. *IEEE Transactions on Circuits and Systems for Video Technology*, 2019. [2](#), [7](#), [11](#)
- [47] Daniel Stadler and Jurgen Beyerer. Improving multiple pedestrian tracking by track management and occlusion handling. In *Proceedings of the IEEE/CVF Conference on Computer Vision and Pattern Recognition (CVPR)*, pages 10958–10967, June 2021. [7](#), [11](#)
- [48] Russell Stewart, Mykhaylo Andriluka, and Andrew Y Ng. End-to-end people detection in crowded scenes. In *Proceedings of the IEEE conference on computer vision and pattern recognition*, pages 2325–2333, 2016. [2](#), [5](#)
- [49] Siyu Tang, Mykhaylo Andriluka, Bjoern Andres, and Bernt Schiele. Multiple people tracking by lifted multicut and person re-identification. In *IEEE Conf. Comput. Vis. Pattern Recog.*, 2017. [2](#)
- [50] Pavel Tokmakov, Jie Li, Wolfram Burgard, and Adrien Gaidon. Learning to track with object permanence. In *Int. Conf. Comput. Vis.*, 2021. [2](#), [7](#)
- [51] Ashish Vaswani, Noam Shazeer, Niki Parmar, Jakob Uszkoreit, Llion Jones, Aidan N Gomez, Łukasz Kaiser, and Illia Polosukhin. Attention is all you need. In *Adv. Neural Inform. Process. Syst.*, 2017. [1](#), [2](#), [3](#), [4](#), [9](#)
- [52] Paul Voigtlaender, Michael Krause, Aljosa Osep, Jonathon Luiten, Berin Balachandar Gnana Sekar, Andreas Geiger, and Bastian Leibe. Mots: Multi-object tracking and segmentation. In *IEEE Conf. Comput. Vis. Pattern Recog.*, 2019. [2](#), [6](#), [7](#), [8](#), [9](#), [11](#), [13](#)
- [53] Qiang Wang, Yun Zheng, Pan Pan, and Yinghui Xu. Multiple object tracking with correlation learning. In *IEEE Conf. Comput. Vis. Pattern Recog.*, 2021. [7](#)
- [54] Shuai Wang, Hao Sheng, Yang Zhang, Yubin Wu, and Zhang Xiong. A general recurrent tracking framework without real data. In *Int. Conf. Comput. Vis.*, 2021. [7](#)
- [55] Yongxin Wang, Kris Kitani, and Xinshuo Weng. Joint object detection and multi-object tracking with graph neural networks. In *IEEE Int. Conf. Rob. Aut.*, May 2021. [2](#), [7](#)
- [56] Yuqing Wang, Zhaoliang Xu, Xinlong Wang, Chunhua Shen, Baoshan Cheng, Hao Shen, and Huaxia Xia. End-to-end video instance segmentation with transformers. In *Proc. IEEE Conf. Computer Vision and Pattern Recognition (CVPR)*, 2021. [6](#), [9](#)
- [57] Jialian Wu, Jiale Cao, Liangchen Song, Yu Wang, Ming Yang, and Junsong Yuan. Track to detect and segment: An online multi-object tracker. In *Proceedings of the IEEE Conference on Computer Vision and Pattern Recognition*, 2021. [2](#), [7](#)
- [58] Zhenbo Xu, Wei Zhang, Xiao Tan, Wei Yang, Huan Huang, Shilei Wen, Errui Ding, and Liusheng Huang. Segment as points for efficient online multi-object tracking and segmentation. In *Eur. Conf. Comput. Vis.*, 2020. [2](#), [7](#), [8](#)

- [59] Kota Yamaguchi, Alexander C. Berg, Luis E. Ortiz, and Tamara L. Berg. Who are you with and where are you going? *IEEE Conf. Comput. Vis. Pattern Recog.*, 2011. [2](#)
- [60] Fan Yang, Xin Chang, Sakriani Sakti, Yang Wu, and Satoshi Nakamura. Remot: A model-agnostic refinement for multiple object tracking. *Image and Vision Computing*, 106:104091, 2021. [7](#)
- [61] Fan Yang, Wongun Choi, and Yuanqing Lin. Exploit all the layers: Fast and accurate cnn object detector with scale dependent pooling and cascaded rejection classifiers. *IEEE Conf. Comput. Vis. Pattern Recog.*, 2016. [6](#), [10](#), [12](#), [13](#)
- [62] Fan Yang, Wongun Choi, and Yuanqing Lin. Exploit all the layers: Fast and accurate cnn object detector with scale dependent pooling and cascaded rejection classifiers. *IEEE Conf. Comput. Vis. Pattern Recog.*, pages 2129–2137, 2016. [8](#)
- [63] Qian Yu, Gerard Medioni, and Isaac Cohen. Multiple target tracking using spatio-temporal markov chain monte carlo data association. *IEEE Conf. Comput. Vis. Pattern Recog.*, 2007. [2](#)
- [64] Li Zhang, Yuan Li, and Ramakant Nevatia. Global data association for multi-object tracking using network flows. *IEEE Conference on Computer Vision and Pattern Recognition (CVPR)*, 2008. [2](#)
- [65] Y. Zhang, H. Sheng, Y. Wu, S. Wang, W. Lyu, W. Ke, and Z. Xiong. Long-term tracking with deep tracklet association. *IEEE Trans. Image Process.*, 2020. [2](#), [7](#), [11](#)
- [66] Yifu Zhang, Chunyu Wang, Xinggang Wang, Wenjun Zeng, and Wenyu Liu. Fairmot: On the fairness of detection and re-identification in multiple object tracking. *International Journal of Computer Vision*, pages 1–19, 2021. [7](#)
- [67] Liang Zheng, Liyue Shen, Lu Tian, Shengjin Wang, Jingdong Wang, and Qi Tian. Scalable person re-identification: A benchmark. In *Int. Conf. Comput. Vis.*, 2015. [7](#)
- [68] Linyu Zheng, Ming Tang, Yingying Chen, Guibo Zhu, Jinqiao Wang, and Hanqing Lu. Improving multiple object tracking with single object tracking. In *IEEE Conf. Comput. Vis. Pattern Recog.*, pages 2453–2462, 2021. [7](#)
- [69] Xingyi Zhou, Vladlen Koltun, and Philipp Krähenbühl. Tracking objects as points. *ECCV*, 2020. [1](#), [2](#), [5](#), [6](#), [7](#), [8](#), [9](#), [11](#), [13](#)
- [70] Ji Zhu, Hua Yang, Nian Liu, Minyoung Kim, Wenjun Zhang, and Ming-Hsuan Yang. Online multi-object tracking with dual matching attention networks. In *Eur. Conf. Comput. Vis.*, 2018. [1](#), [2](#)
- [71] Xizhou Zhu, Weijie Su, Lewei Lu, Bin Li, Xiaogang Wang, and Jifeng Dai. Deformable detr: Deformable transformers for end-to-end object detection. *Int. Conf. Learn. Represent.*, 2021. [2](#), [6](#), [9](#)